Published in final edited form as:
Nanomedicine. 2015 January ; 11(1): 109–118. doi:10.1016/j.nano.2014.08.001.

Graphene Nanoribbons as a Drug Delivery Agent for Lucanthone Mediated Therapy of Glioblastoma Multiforme

Sayan Mullick Chowdhury[2,#], **Cassandra Surhland**[2,#], **Zina Sanchez**[1], **Pankaj Chaudhary**[3], **M.A. Suresh Kumar**[1], **Stephen Lee**[2], **Louis A. Peña**[2,4], **Michael Waring**[5], **Balaji Sitharaman**[2,*], and **Mamta Naidu**[6,*]

[1]Department of Pharmacological Sciences, Stony Brook University, NY

[2]Department of Biomedical Engineering, Stony Brook University, Stony Brook, NY

[3]Centre for Cancer Research and Cell Biology, Queens University Belfast, UK

[4]Biosciences Department, Brookhaven National Laboratory, NY

[5]Department of Pharmacology, Tennis Court Road, Cambridge University, UK

[6]GeneSys Research Institute/Center for Cancer Systems Biology at Tufts School of Medicine, Boston, MA

Abstract

We report use of PEG-DSPE coated oxidized graphene nanoribbons (O-GNR-PEG-DSPE) as agent for delivery of anti-tumor drug Lucanthone (Luc) into Glioblastoma Multiformae (GBM) cells targeting base excision repair enzyme APE-1 (Apurinic endonuclease-1). Lucanthone, an endonuclease inhibitor of APE-1, was loaded onto O-GNR-PEG-DSPEs using a simple non-covalent method. We found its uptake by GBM cell line U251 exceeding 67% and 60% in APE-1-overexpressing U251, post 24 hours (h). However, their uptake was ~38% and 29% by MCF-7 and rat glial progenitor cells (CG-4), respectively. TEM analysis of U251 showed large aggregates of O-GNR-PEG-DSPE in vesicles. Luc-O-GNR-PEG-DSPE was significantly toxic to U251 but showed little / no toxicity when exposed to MCF-7/CG-4 cells. This differential uptake effect can be exploited to use O-GNR-PEG-DSPEs as a vehicle for Luc delivery to GBM, while reducing nonspecific cytotoxicity to the surrounding healthy tissue. Cell death in U251 was necrotic, probably due to oxidative degradation of APE-1.

[*]Address Correspondence to: For Thioxanthenones, APE-1, GBM and CG-4 studies, Mamta Naidu, PhD, Associate Investigator/Asst. Professor of Medicine, GeneSys Research Institute/Center for Cancer Systems Biology, Tufts University School of Medicine, Boston, MA 02135, Tel: 617-779-3010, mamta.naidu@steward.org. For Graphene Nanoribbons, Balaji Sitharaman, PhD, Assistant Professor of Biomedical Engineering, Stony Brook University, Stony Brook, NY 11794, Tel: 631-632-1810, balaji.sitharaman@stonybrook.edu.
[#]Equal contributors

Introduction

APE-1, the primary base excision repair (BER) enzyme of mammalian system is over-expressed in a variety of tumors[1]. Although there is evidence both for and against a correlation between APE-1 levels and radioresistance in tumors [2], an inverse relationship between the expression level of APE-1 and radiation and chemotherapy responses has been observed in medulloblastoma and primitive neuroectodermal tumors [3]. *In vitro* studies have also shown that APE-1 contributes to the glioma cell resistance in response to alkylating agents therapy, and its endonuclease activity is increased by oxidative stress [4]. Previously, we[5] and others [6, 7] had demonstrated a correlation between base excision repair protein APE-1 and radiation sensitivity with GBM cell cultures. Also, we have shown that thioxanthenones such as lucanthone (CAS 479-50-5) and hycanthone (CAS 3105-97-3) inhibit the APE-1 endonuclease function in GBM cell lines with higher or overexpressed APE-1 levels without affecting its DNA substrate binding function [8]. As the next step, it is essential to determine whether we can use this mechanistic insight to cause tumor regression in mouse tumor models. However, as APE-1 is present both in normal and tumor cells, a way to target these thioxanthenones to GBM and other tumors specifically with no/minimal damage to the surrounding normal tissue is needed.

Graphene, a two dimensional, single layer, hexagonal lattice of carbon atoms has attracted much attention due to its unique chemical and physical properties [9]. Studies have also established that graphene can be used in various biomedical applications such as imaging and drug delivery [10–12]. The large surface of graphene can be chemically modified with a wide variety of molecules that can enhance biocompatibility [13], solubility [14], or allow the targeting to specific cell types and hence proves to be a good platform for biomedical use [15]. Reports show that oxidized graphene nanoplatelets synthesized by modified Hummer's method (chemical oxidation of graphite followed by ultrasonic cleavage) and coated with the amphiphilic polymer 1,2-distearoyl-*sn*-glycero-3-phosphoethanolamine-N-[amino(polyethylene glycol (DSPE-PEG) can load high amounts of aromatic molecules such as the drug doxorubicin and release them into tumor cells [14, 16]. The loading of the drug is achieved through the pi-stacking, a non-covalent interaction between electrons in adjacent pi bonds [14, 16].

Recently, Kosynkin, Tour, and co-workers have pioneered a method that allows the synthesis of oxidized graphene nanoribbons (O-GNRs) in macroscopic amounts by the longitudinal unzipping of multi walled carbon nanotubes [17]. Our recent *in vitro* studies indicate that these nanoparticles coated with PEG-DSPE (hereafter called O-GNR-PEG-DSPE) may also be suitable for cell specific drug delivery [18]. In this paper, we report the efficacy of O-GNR-PEG-DSPE to load and deliver Luc to the GBM cell line U251.

Materials & Methods

Reagents

Cell Line U251 and reagents used for measuring endonuclease activity were as described previously [8]. CG-4, rat glial progenitor cell line that remains a progenitor for only about 20–25 passages was kind gift from Dr. Toru Ogata from Research Institute, Namiki,

Tokorozawa-City, Japan. Luc obtained from Dr. S. Archer (Sterling-Winthrop Research Institute, Rensselaer, NY) were maintained at 4°C under hygroscopic conditions, and dissolved in 1.2 mg/mL PEG-DSPE (in double distilled water) just prior to reactions. Plasmids consisting of full length APE-1 in pCMV10 were a kind gift from Dr. Bruce Demple (Stony Brook University, NY). Multi-walled carbon nanotubes and propidium iodide (PI) were obtained from Sigma Aldrich. All cell culture components were obtained from GIBCO. Annexin V /PI staining kits were obtained from Trevigen.

Cell Culture

U251 transfected with either the blank plasmid pCMV10 (CMV/U251) or full length APE-1 in pCMV10 (AI-5/CMV/U251) were grown in Dulbecco's Modified Eagle Medium (DMEM) supplemented with 10% fetal bovine serum and 800 μg/ml of G418. CG-4 were grown in 70% of DMEM F12 containing 1X penicillin-streptomycin (100 ug/ml Streptomycin + 100U of penicillin) (PS) with 1X N2 supplement (containing 1 mM Transferrin, 0.06 mM Insulin, 0.002 mM progesterone, 10 mM putresceine and 0.003 mM selenite) and 30% of B104 conditioned medium. MCF-7 were grown at 37°C in a humidified atmosphere of 5% CO_2 in RPMI medium supplemented with 10% fetal bovine serum and 1X PS.

O-GNR Synthesis

O-GNRs were synthesized from multi-walled carbon nanotubes (MWCNTs)(Sigma-Aldrich, Length=5–9 μm) using the oxidative longitudinal unzipping method [17]. Briefly, MWCNTs (150 mg) were suspended in 30 ml concentrated (96%) H_2SO_4. After 4 h, 4.75 mM $KMnO_4$ was added slowly and stirred for an h followed by further stirring for another h at 55–70 °C in an oil bath. This solution was poured on ice (400 ml) containing 5mL 30% H_2O_2 and the ice-H_2O_2 slurry was allowed to melt. The solution obtained was centrifuged at 3000 rpm for 30 minutes, after which the supernatant was discarded. The pellet obtained was then washed with 36% HCl. Ethanol and ether washes were used for flocculation and the final product (O-GNR) was obtained as pellet after centrifugation (30 minutes, 3000 rpm). This product was dried overnight in a vacuum oven at 60°C.

O-GNRs were characterized using atomic force microscopy (AFM) and Transmission Electron Microscopy (TEM). AFM images were obtained using a Nano Surf Easy Scan 2 AFM (NanoScience Instruments Inc, Phoenix, AZ) operating in tapping mode using a V-shaped cantilever and TEM images were obtained using a Tecnai Bio Twin G transmission electron microscope (FEI, Hillsboro, OR), at 80 kV.

Luc loading on O-GNR-PEG-DSPE

Powdered O-GNRs were dispersed in a solution of 1.2mg/mL 1, 2-distearoyl-*sn*-glycero-3-phosphoethanolamine-N-[amino (polyethylene glycol)) (PEG-DSPE), at a concentration of 1 mg/mL. This dispersion was bath sonicated for 30 minutes to produce O-GNR-PEG-DSPE. 1 mg/mL solution of Luc in 1.2 mg/mL PEG-DSPE served as a Luc stock solution. 200 μL of the O-GNR-PEG-DSPE solution and 400 μL of the Luc solution were combined in a 20 mL glass vial, and the total volume was made up to 1 mL using a stock solution of 1.2 mg/mL PEG-DSPE and stirred at 4 °C for 24 hrs. After this loading period, unincorporated

Luc was separated out from the loaded O-GNRs by centrifugation at 13000 RPM for 1 hour. In order to calculate the loading efficiency, the absorbance of the supernatant was measured at 328 nm using an Evolution 300 UV-Vis Spectrophotometer (Thermo Fisher Scientific, Waltham, MA) and compared to a standard curve. The loading efficiency was calculated by subtracting the unloaded Luc from the total available Luc. Loaded O-GNR-PEG-DSPEs were left in pellet form until used.

Uptake of O-GNR-PEG-DSPE in the U251 and CG-4 cell lines (using flow cytometry)

O-GNR-PEG-DSPEs were loaded with PI and purified using the same method used for Luc loading. CMV/U251 and A1-5/CMV/U251 were grown in 10 cm dishes at 37 °C and 5% CO_2 in DMEM. Cells were either incubated with PI-loaded O-GNR-PEG-DSPEs at a concentration of 40 μg per mL (previously reported to be a non-toxic concentration) (15) of media, or left untreated. After 24 h, cells were trypsinized, resuspended in FACS buffer (1X PBS containing 20% fetal bovine serum) and placed on ice. Flow cytometry was performed immediately after all samples were prepared using a FACS Calibur Cell Sorter (BD Biosciences, San Jose, CA).

Transmission Electron Microscopy

Six well plates with surfaces covered with ACLAR® film (Electron Microscopy Sciences, Hatford, PA) were plated with CMV/U251 and MCF-7 cells at a density of 5×10^5 cells per plate, and exposed to O-GNR-PEG-DSPE for 3 h. At the end of 3 h, cells were fixed with 2.5% electron microscopy grade glutaraldehyde (Electron Microscopy Sciences, Hatford, PA) in 1X PBS. After fixation, the films containing fixed cells were placed in 2% osmium tetroxide in 1X PBS, dehydrated through graded ethanol washes, and embedded in durcupan resin (Sigma-aldrich, St. Louis, USA). Areas with high cell densities were blocked, cut into 80 nm ultra-thin sections using an Ultracut E microtome (Reichert-Jung, Cambridge, UK), and placed on formvar-coated copper grids. The sections were then viewed with a Tecnai Bio Twin G transmission electron microscope (FEI, Hillsboro, OR), at 80 kV. Digital images were acquired using an XR-60 CCD digital camera system (AMT, Woburn, MA).

Presto Blue Assay

In separate cultures—Luc alone (80μM), 80 μM Luc loaded O-GNR-PEG-DSPE and O-GNR-PEG-DSPE (same weight as used for Luc loading) were incubated with CMV/U251, A1-5/CMV/U251, MCF-7 and CG-4 cells (5×10^3 cells per well in 96 well plates) for 24 h. Following the incubation period the media was removed and the cells were washed twice with 1X PBS. 100 μL of fresh media was added to each well and 10 μl of Presto Blue reagent was added to it and incubated for 4 h. Fluorescence was measured by Cytofluor fluorescence multiwell plate reader (Infinite M200, Tecan Group Ltd, NC, USA) with excitation at 530 nm, and emission at 580 nm. The cell viability in terms of % of unexposed cells is expressed as the percentage of $(F_{test} - F_{blank})/(F_{control} - F_{blank})$, where F_{test} is the fluorescence of the cells exposed to nanoribbon-drug sample, $F_{control}$ is the fluorescence of the untreated sample and F_{blank} is the fluorescence of the wells without any cells. The presto blue reading for all lysed cells was also taken for comparison.

MCF-7-CMV/U251 and CG-4-CMV/Co-Culture—MCF-7, CG-4 and CMV/U251 were seeded separately on 12mm round glass coverslips (Fisherbrand, Fisher Scientific, PA, USA) in 100mm plates at a density of 2.2×10^6 cells and allowed to grow overnight. For the two separate co-culture condition experiments, one coverslip from each cell line was placed in 6 well plates, for a total of two coverslips per well. These cells were then incubated with Luc alone (80μM), 80 μM Luc loaded O-GNR-PEG-DSPE or O-GNR-PEG-DSPE for 24 h. After the incubation period, the media was removed and the cells were washed twice with 1X PBS. Each coverslip was then transferred to its own well in 6 well plates containing 3mL of media and 300μL of Presto Blue reagent. After incubating for 4 h, the fluorescence intensity was recorded using the procedure described above.

Annexin V/PI staining—Luc alone and Luc-loaded O-GNR-PEG-DSPEs at different concentrations (5–80 μM) were incubated with CMV/U251, A1-5/CMV/U251 and CG-4 (5×10^5 cells/3ml in 6-well plates) for 4 h. Unexposed cells were used as control. Unloaded O-GNR-PEG-DSPEs in amounts equivalent to the loaded nanoparticles were also exposed to all the cell types as delivery agent control. The viability of the cells was analyzed by flow cytometry after Annexin V/PI staining using FACS Calibur Cell Sorter (BD Biosciences, San Jose, CA).

Statistics

Presto blue data is presented as mean ± standard deviation (n = 6). Student 't' test was used to analyze the differences among groups. One-way ANOVA followed by Tukey Kramer post hoc analysis was used for multiple comparisons between groups. All statistical analyses were performed using a 95% confidence interval ($p < 0.05$).

Results

AFM and TEM analysis of O-GNRs

Figure 1A and B shows representative AFM and TEM images of the O-GNRs. The O-GNRs are thin, elongated strips of graphene that possess straight edges with an average breadth of 100–300 nm and length of 500–2500 nm as determined from six different AFM images. Figure 1A shows two unzipped nanoribbons with lengths ~500 nm each. Figure 1B shows multiple unzipped nanoribbons with lengths between 1000 to 2500 nm.

Luc loading on O-GNRs

Using a standard curve of Luc, and employing a previously determined ideal ratio of 1:1.5 of Luc: O-GNR it was determined that O-GNR-PEG-DSPE could load 310 μM of Luc per mg (Figure S1). For a schematic of the loading process, see Figure 1C.

Uptake of O-GNR-PEG-DSPEs in U251 cells

PI is a DNA intercalating fluorescent dye that it is normally excluded from live cells. However, when conjugated to a delivery agent such as O-GNR-PEG-DSPE it can enter live, intact cells. Figure 2 showing the flow cytometry analysis of U251 and CG-4 incubated with PI loaded O-GNR-PEG-DSPE revealed that ~60 % of A1-5/CMV/U251 showed uptake of

PI-loaded O-GNR-PEG-DSPEs, while ~67 % of CMV/U251 showed uptake. However, only ~38% of MCF and ~29% of CG-4 showed uptake of the PI loaded O-GNR-PEG-DSPE.

TEM

Figure 3A and B show that CMV/U251 could take up large aggregates of O-GNR-PEG-DSPE into large vesicular structures (black arrows) that localized near the nucleus (yellow arrows). Figure 3C shows that MCF did not show uptake of large aggregates although few small aggregates were observed (black arrow). Figure 3D shows that large aggregates of O-GNR-PEG-DSPE on the surface of MCF-7 (black arrow) failed to get taken up by MCF-7.

MCF-7-CMV/U251 and CG-4-CMV/U251 Co-Cultures

Figure 3E shows that MCF-7 and CMV/U251 treated with 80 μM Luc exhibit a viability of ~36% and ~28% respectively when compared to untreated controls. CMV/U251 still exhibited significant decreased viability when exposed to Luc-loaded O-GNR-PEG-DSPE, with only ~56% viability compared to untreated control. However, MCF-7 exposed to Luc-loaded O-GNR-PEG-DSPE do not exhibit decreased viability compared to untreated controls. O-GNR-PEG-DSPE alone was not toxic to either cell line. This trend held true for the CG-4 and CMV/U251 co-culture also (Figure 3F). CG-4 and CMV/U251 treated with 80 μM Luc exhibit a viability of ~30% and ~15% respectively when compared to untreated controls. CMV/U251 exhibited significant decreased viability when exposed to Luc-loaded O-GNR-PEG-DSPE, with only ~29% viability compared to untreated control. However, CG-4 exposed to Luc-loaded O-GNR-PEG-DSPE showed ~78% viability compared to untreated controls, although this difference was not statistically significant.

Presto Blue assay to assess cell death

Presto Blue is a resazurin dye based cell viability assay in which healthy cells with normal metabolic activity and mitochondrial integrity can convert resazurin in the assay reagent to a pink fluorescent dye. The amount of non-fluorescence to fluorescence conversion is directly proportional to the number of healthy cells present. Figure 4A and Figure 4B shows that CMV/U251 and A1-5/CMV/U251 show a viability of ~40% and ~ 30% compared to untreated controls when exposed to 80μM of free Luc which changes to ~70% viability for both cell lines when the drug is loaded onto O-GNR-PEG-DSPE. Figure 4C and Figure 4D show that compared to untreated cells, CG-4 and MCF-7 do not show statistically significant toxicity when exposed to 80μM Luc loaded O-GNR-PEG-DSPE.

Annexin V/PI staining of U251 cells exposed to free or loaded drug

Annexin V (AV) is a 35 KDa phospholipid binding protein with a high affinity for phospatidyl serine[19]. Early apoptotic cells show exposed phosphotidyl serine on their cell surface while it is still intact. PI on the other hand can only enter dead cells or early necrotic cells with compromised membranes. Thus, in flow cytometry AV +/PI+ represents dead cells, AV+/PI− represents cells in early apoptosis, AV−/PI+ represents dead or necrotic cells with compromised membranes, and AV−/PI− represents healthy living cells. Flow cytometry of CMV/U251 exposed to 5–80 μM Luc showed a concentration dependent decrease in AV−/PI− cells with no healthy living cells remaining after 4 h of exposure to 80

μM of the drug. However, 37% of cells were still living after 4 h of exposure to O-GNR-PEG-DSPE loaded with 80μM Luc. APE-1 overxpressing AI-5/CMV/U251 also showed a concentration dependent decrease in cell viability with 100% cell death occurring at 40 μM exposure for 4 h. However, exposure of these cells to Luc loaded nanoparticles showed 56% and 43% of the exposed cells were still living after 4 h of exposure to O-GNR-PEG-DSPE loaded with 40μM and 80μM Luc respectively. Exposure of the cells to different amounts of nanoparticles by themselves did not show significant toxicity either (Figure S2). Flow cytometry data also indicated that dead cells were mainly PI+/AV- in nature (Figure 5).

Discussion

The efficient delivery of thioxanthanones like Luc and its analogues to GBM tumors for effective inhibition of overexpressed APE-1 requires a drug delivery agent that is stable in aqueous solutions, loads high concentrations of the drug, and can be easily taken up by the tumor cells. Also, there should be a slow, sustained and controlled release of the drug so as to decrease the non-specific release of the drug before reaching its target site. Most importantly, the agent should be easy to functionalize by targeting groups so that the efficiency of targeting can be improved. A recent review by Zhou *et al* [20] elegantly presents updates on novel strategies for GBM therapy, delineating those where nanoparticles are introduced systemically, where this approach has been working some times, but the percentage of intravenously administered particles that enter the brain is very low[21]. It is not yet clear whether enough of the drug can be delivered by systemically-administered nanoparticles for treating tumors in the brain, although there is some evidence that systemically-administered nanoparticles are useful for diagnostic purposes, such as iron oxide-containing nanoparticles that facilitate imaging of brain tumors[22]. Another approach has delivered the nanoparticles directly into the brain, perhaps using Convection enhanced delivery (CED) to facilitate the distribution of the nanoparticles throughout the volume of the brain that needs therapy[23].

O-GNRs with their large surface area provide a suitable platform for loading Luc through pi stacking interactions. The non-covalent coating of PEG-DSPE on the O-GNRs also ensures that they are stable in aqueous suspension. We could load as high 310 μM of Luc onto each milligram of O-GNR-PEG-DSPE. Other thioxanthanones (Hycanthone, and its structural analogue Inadazole-6 (IA-6) with similar structure are expected to have similar loading efficiency on O-GNR-PEG-DSPE.

We have recently shown that O-GNR-PEG-DSPEs show differential uptake based on cell type and thus cannot be taken up by all cells [18]. This is probably due to the fact that O-GNR-PEG-DSPEs are relatively large sized nanoparticles (between 0.5–2.5 μm in length, Figure 1). As such, it is likely that they are taken up by specialized receptor mediated uptake mechanisms or by macropinocytotic mechanisms[24]. Flow cytometry based analysis showed that ~ 67% of CMV/U251 and ~60% of A1-5/CMV/U251 cells showed presence of these particles after 24 h proving that these particles get taken up by U251 (Figure 2). This could be due to the presence of specific receptors on the surface of U251 that promote uptake of these particles through receptor mediated endocytosis or induce a macropinocytotic response as we had reported before for uptake of these particles in HeLa

cells [18]. In comparison only ~ 38% of MCF-7 and ~29% of CG-4, showed presence of O-GNR-PEG-DSPE in them indicating that these particles have a cell specific higher uptake in the GBM cell lines (Figure 2).

One major objective for targeted drug delivery of Luc is to decrease the side effects caused by unwanted uptake of Luc by normal tissue. Unwanted uptake of Luc can be prevented if the drug delivery agent has an inherent low uptake in normal tissue and enhanced with slower release of the drug slowly so that once injected intravenously they will release the maximum load of drug only after being taken up by the tumor. TEM images of CMV/U251 showed that these cells could take up large aggregates whereas MCF-7/CG-4 failed to do so resulting in accumulation of large O-GNR-PEG-DSPE aggregates on the surface (Figure 3). This further indicates that CMV/U251 might have some specialized mechanism for the uptake of larger O-GNR-PEG-DSPE aggregates. Uptake of large aggregates would mean better drug delivery and hence more efficient APE-1 inhibition in CMV/U251. Presto Blue assay of the four cell lines (U251, A1-5/U251, MCF-7 and CG-4) exposed to free Luc (80 μM) and Luc(80μM) loaded on O-GNR-PEG-DSPE showed that loading decreased the toxicity of Luc by ~ 30% in U251 cells and ~ 40% in APE-1 overexpressing U251 cells compared to free drug (Figure 4). However, the cell death observed in the drug loaded nanoparticles was significantly higher compared to unexposed cells (Figure 4). Luc loaded O-GNR-PEG-DSPE did not show high toxicity in CG-4 and MCF-7 cells although the free drug was toxic to them, due to lower uptakeof Luc- O-GNR-PEG-DSPE uptake in these cells (Figure 2). This differential uptake phenomenon held true even when MCF-7 and CMV/U251 cells were exposed to Luc-O-GNR-PEG-DSPE together as co-culture. Although CMV/U251 exposed to 80μM Luc loaded on O-GNR-PEG-DSPE exhibited only ~56% viability compared to untreated control, MCF-7 exposed to Luc-loaded O-GNR-PEG-DSPE in the same wells as CMV/U251 did not show significantly reduced viability compared to untreated controls (Figure 3E). This differential uptake and toxicity was further confirmed when CG-4 also showed much lower toxicity compared to CMV/U251 in co-culture (Figure 3F). Taken together, the TEM images and cell viability experiments indicate that U251 have higher uptake of drug loaded O-GNR-PEG-DSPE and hence shows higher cell death.

To test the mechanism of cell death induced by the drug loaded onto O-GNR-PEG-DSPE we compared the effect of different concentrations (5–80 μM) of free Luc and Luc loaded onto nanoparticles, when exposed for 4 h to CMV/U251 and AI-5/CMV/U251 using Annexin V/PI staining. As expected the U251 were sensitive to the free Luc with 100% cell death observed at 80μM in CMV/U251 and 40 μM free drug concentration in AI-5/CMV/U251. The A1-5 overexpressor was more sensitive to free Luc most likely owing to about 35 fold higher expression of APE-1 in this overexpressor U251 clone[5]. Exposure of CMV/U251 to Luc loaded O-GNR-PEG-DSPE showed an increase in cell viability by ~64% at 5μM and ~37% at 80μM (Figure 4). Similarly, APE-1 overexpressing AI-5/CMV/U251 showed an increase in cell viability by 53% at 5 μM and ~43% at 80 μM (Figure 4) of loaded drug compared to free drug at the same concentrations. We also compared the toxicity of various weights of O-GNR-PEG-DSPE used to load 5-80 μM Luc on CMV/U251. O-GNR-PEG-DSPE showed negligible toxicity at all weights tested proving that the toxicity observed was primarily due to the released Luc. This also indicated that loading Luc onto O-GNR-PEG-DSPE does not affect its activity and thus the decrease in cell death may

be due to the lower uptake of particles or slower release of Luc from O-GNR-PEG-DSPE. To ensure this differential toxicity observed is not due to lesser uptake of the O-GNR-PEG-DSPE particles we repeated the toxicity based drug delivery experiments on HeLa cells which we have previously shown to be able take up these particles [18]. Analysis of presto blue cell viability assay showed that cell death observed after 24 h of exposure to 3.1 μM of Luc loaded onto O-GNR-PEG-DSPE was significantly lesser than both 1.55 μM (50% of loaded) and 3.1 μM (same as loaded) of free drug showing that the decrease in toxicity observed was not due to low uptake of nanoparticles (Figure S3). Thus we hypothesize that the decrease in cell death observed in drug loaded O-GNR-PEG-DSPE may be due to slower release of the drug from the particles. Further experiments are needed to confirm this hypothesis. Another important observation from Annexin V/PI results was that almost all the dead cells exposed to either free drug or drug loaded onto O-GNR-PEG-DSPE were PI +/AV- suggesting that the cell death was necrotic (Figure 5). Necrotic cell death is generally triggered by external factors or factors that cause damage to internal functioning of the cell through generation of stress and ultimately breakdown of cellular machinery [25]. We had reported earlier that Luc leads to an oxidative stress mediated degradation of APE-1 which might be causing the necrosis-mediated death observed [8].

Although, O-GNR-PEG-DSPE has been shown to be taken up only by certain cell types [18], we can also functionalize it with groups that can increase their targeting efficiency to tumors. Such functionalization for the purpose of targeting have been reported previously for smaller graphene oxide nanoplatelets which are synthesized using Hummers method [26]. O-GNR-PEG-DSPE, with its large surface area can be similarly functionalized with antibodies targeting different tumors. The basis of functionalization is often to target receptors over-expressed on cancer cells using antibodies or groups that can bind to these receptors. For example, graphene oxide particles functionalized with antibodies against folate receptors have been used to target them to cancer cells over expressing folate receptors [26–28]. O-GNR-PEG-DSPE functionalized with antibodies against epidermal growth factor receptors which are often over expressed in GBM tumors can be utilized to increase their targeting to these tumors [29]. However, functionalization often leads to decreased drug loading efficiencies due to decrease in surface area available for drug loading.

Thus overall O-GNR-PEG-DSPE can be considered a good vessel for delivering Luc to GBM tumors. However, its further development as a drug delivery agent can take place only after optimization of efficacy, drug release kinetics and uptake in multiple tumor models and cell lines (GBM, neuroblastoma, prostate tumors, neural progenitor cell lines etc) have been completed. Our future research will also focus on the release kinetics of Luc from O-GNR-PEG-DSPEs to ensure prolonged suppression of the tumors. This will include studies that explore the pH dependency of drug release *in vitro*. Once we have established a clear kinetics for death of GBM cells through delayed release of Luc, we will use these Luc-loaded O-GNR-PEG-DSPEs for targeted delivery to orthotopic GBM tumors in mice.

Supplementary Material

Refer to Web version on PubMed Central for supplementary material.

Acknowledgments

This work was supported by DOE grant to LP (DOE grant KP-1401020/MO-079) and NIH grant to SB (1DP2OD007394-01). We wish to thank the Transmission Electron Microscopy (TEM) Facility, under the direction of Susan C. Van Horn, in the Central Microscopy Imaging Center (C-MIC) at Stony Brook University, Stony Brook, New York 11794 for their contribution towards the TEM preparation and data collection.

References

1. Bobola MS, Finn LS, Ellenbogen RG, Geyer JR, Berger MS, Braga JM, et al. Apurinic/apyrimidinic endonuclease activity is associated with response to radiation and chemotherapy in medulloblastoma and primitive neuroectodermal tumors. Clin Cancer Res. 2005; 11:7405–14. [PubMed: 16243814]
2. Evans AR, Limp-Foster M, Kelley MR. Going APE over ref-1. Mutat Res. 2000; 461:83–108. [PubMed: 11018583]
3. Bobola MS, Finn LS, Ellenbogen RG, Geyer JR, Berger MS, Braga JM, et al. Apurinic/apyrimidinic endonuclease activity is associated with response to radiation and chemotherapy in medulloblastoma and primitive neuroectodermal tumors. Clin Cancer Res. 2005; 11:7405–14. [PubMed: 16243814]
4. Silber JR, Bobola MS, Blank A, Schoeler KD, Haroldson PD, Huynh MB, et al. The Apurinic/Apyrimidinic Endonuclease Activity of Ape1/Ref-1 Contributes to Human Glioma Cell Resistance to Alkylating Agents and Is Elevated by Oxidative Stress. Clinical Cancer Research. 2002; 8:3008–18. [PubMed: 12231548]
5. Naidu MD, Mason JM, Pica RV, Fung H, Pena LP. Radiation resistance in glioma cells determined by DNA damage repair activity of Ape1/Ref-1. Japanese Journal of Radiation Research. 2010; 51:393–404.
6. Bobola MS, Blank A, Berger MS, Stevens BA, Silber JR. Apurinic/apyrimidinic endonuclease activity is elevated in human adult gliomas. Clin Cancer Res. 2001; 7:3510–8. [PubMed: 11705870]
7. Jiang Y, Guo C, Fishel ML, Wang Z-Y, Vasko M, Kelley MR. Role of Ape1 in differentiated neurobalstoma SH-SY5Y cells in response to oxidative stress: Use of APE1 small molecule inhibitors to delineated APE1 functions. Aug.2009 11:1273–82.
8. Naidu MD, Agarwal R, Pena LA, Cunha L, Mezei M, Shen M, et al. Lucanthone and Its Derivative Hycanthone Inhibit Apurinic Endonuclease-1 (APE1) by Direct Protein Binding. PLoS ONE. 2011; 6:23679.
9. Allen MJ, Tung VC, Kaner RB. Honeycomb carbon: A review of graphene. Chem Rev. 2010; 110:132–45. [PubMed: 19610631]
10. Zhang Y, Nayak TR, Hong H, Cai W. Graphene: a versatile nanoplatform for biomedical applications. Nanoscale. 2012; 4:3833–42. [PubMed: 22653227]
11. Chowdhury SM, Kanakia S, Toussaint JD, Frame MD, Dewar AM, Shroyer KR, et al. In Vitro Hematological and In Vivo Vasoactivity Assessment of Dextran Functionalized Graphene. Scientific reports. 2013; 3
12. Kanakia S, Toussaint JD, Chowdhury SM, Lalwani G, Tembulkar T, Button T, et al. Physicochemical characterization of a novel graphene-based magnetic resonance imaging contrast agent. International journal of nanomedicine. 2013; 8:2821. [PubMed: 23946653]
13. Kim YK, Kim MH, Min DH. Biocompatible reduced graphene oxide prepared by using dextran as a multifunctional reducing agent. Chemical communications. 2011; 47:3195–7. [PubMed: 21286628]
14. Liu Z, Robinson JT, Sun X, Dai H. PEGylated nanographene oxide for delivery of water-insoluble cancer drugs. Journal of the American Chemical Society. 2008; 130:10876–7. [PubMed: 18661992]
15. Robinson JT, Tabakman SM, Liang Y, Wang H, Casalongue HS, Vinh D, et al. Ultrasmall reduced graphene oxide with high near-infrared absorbance for photothermal therapy. Journal of the American Chemical Society. 2011; 133:6825–31. [PubMed: 21476500]

16. Sun X, Liu Z, Welsher K, Robinson JT, Goodwin A, Zaric S, et al. Nano-Graphene Oxide for Cellular Imaging and Drug Delivery. Nano research. 2008; 1:203–12. [PubMed: 20216934]

17. Kosynkin DV, Higginbotham AL, Sinitskii A, Lomeda JR, Dimiev A, Price BK, et al. Longitudinal unzipping of carbon nanotubes to form graphene nanoribbons. Nature. 2009; 458:872–U5. [PubMed: 19370030]

18. Mullick Chowdhury S, Lalwani G, Zhang K, Yang JY, Neville K, Sitharaman B. Cell specific cytotoxicity and uptake of graphene nanoribbons. Biomaterials. 2013; 34:283–93. [PubMed: 23072942]

19. van Engeland M, Nieland LJW, Ramaekers FCS, Schutte B, Reutelingsperger CPM. Annexin V-Affinity assay: A review on an apoptosis detection system based on phosphatidylserine exposure. Cytometry. 1998; 31:1–9. [PubMed: 9450519]

20. Zhou J, Atsina KB, Himes BT, Strohbehn GW, Saltzman WM. Novel Delivery Strategies for Glioblastoma. Cancer J. 2012; 18:89–99. [PubMed: 22290262]

21. Kreuter J, Ramge P, Petrov V, Hamm S, Gelperina SE, Engelhardt B, et al. Direct evidence that polysorbate-80-coated poly(butylcyanoacrylate) nanoparticles delivery drugs to the CNS via specific mechanisms requiring prior binding of drug to the nanoparticles. Pharm Res. 2003; 20:409–16. [PubMed: 12669961]

22. Kircher MF, Mahmood U, King RS, Weissleder R, Josephson L. A multimodal nanoparticle for preoperative magnetic resonance imaging and intraoperative optical brain tumor delineation. Cancer Res. 2003; 63:8122–5. [PubMed: 14678964]

23. Saito R, Bringas JR, McKnight TR. Distribution of liposomes into brain and rat brain tumor models by convection-enhanced delivery monitored with magnetic resonance imaging. Cancer Res. 2004; 64:2572–9. [PubMed: 15059914]

24. Zhang LW, Monteiro-Riviere NA. Mechanisms of Quantum Dot Nanoparticle Cellular Uptake. Toxicological Sciences. 2009; 110:138–55. [PubMed: 19414515]

25. Zong W-X, Thompson CB. Necrotic death as a cell fate. Genes & Development. 2006; 20:1–15. [PubMed: 16391229]

26. Yang K, Zhang S, Zhang G, Sun X, Lee S-T, Liu Z. Graphene in Mice: Ultrahigh In Vivo Tumor Uptake and Efficient Photothermal Therapy. Nano Letters. 2010; 10:3318–23. [PubMed: 20684528]

27. Yang X, Wang Y, Huang X, Ma Y, Huang Y, Yang R, et al. Multi-functionalized graphene oxide based anticancer drug-carrier with dual-targeting function and pH-sensitivity. Journal of Materials Chemistry. 2011; 21:3448–54.

28. Qin XC, Guo ZY, Liu ZM, Zhang W, Wan MM, Yang BW. Folic acid-conjugated graphene oxide for cancer targeted chemo-photothermal therapy. Journal of Photochemistry and Photobiology B: Biology. 2013; 120:156–62.

29. Heimberger AB, Hlatky R, Suki D, Yang D, Weinberg J, Gilbert M, et al. Prognostic Effect of Epidermal Growth Factor Receptor and EGFRvIII in Glioblastoma Multiforme Patients. Clinical Cancer Research. 2005; 11:1462–6. [PubMed: 15746047]

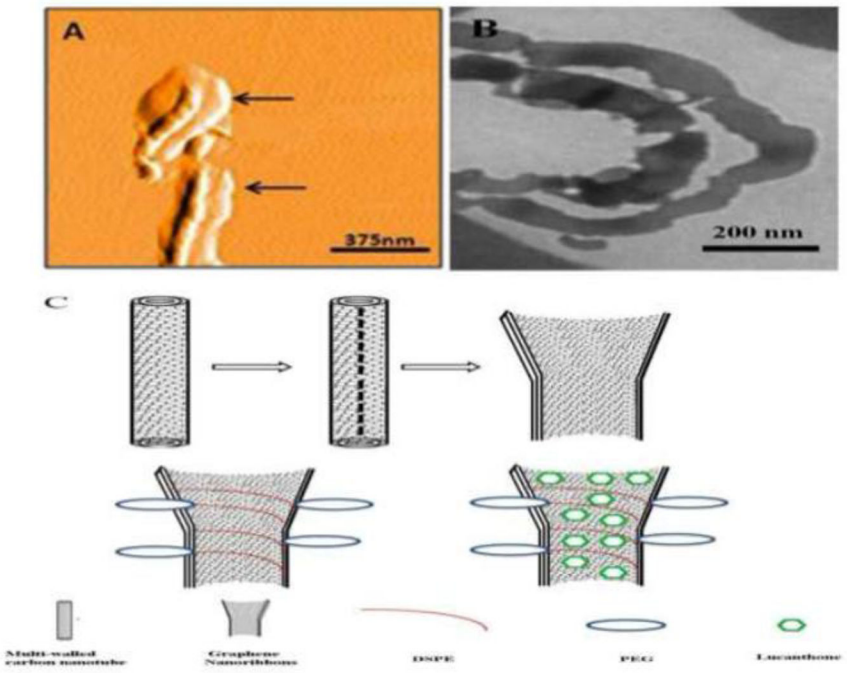

Figure 1.

(A) Representative atomic force microscope (AFM) image of oxidized graphene nanoribbons (O-GNR) showing two completely unzipped O-GNR's ~ 500 nm in length (B) Representative low resolution TEM image of O-GNR showing multiple unzipped O-GNR (C) Schematic showing the unzipping of multi walled tubes to form O-GNR, coating with PEG-DSPE to form O-GNR-PEG-DSPE and loading with lucanthone to form O-GNR-PEG-DSPE-Luc.

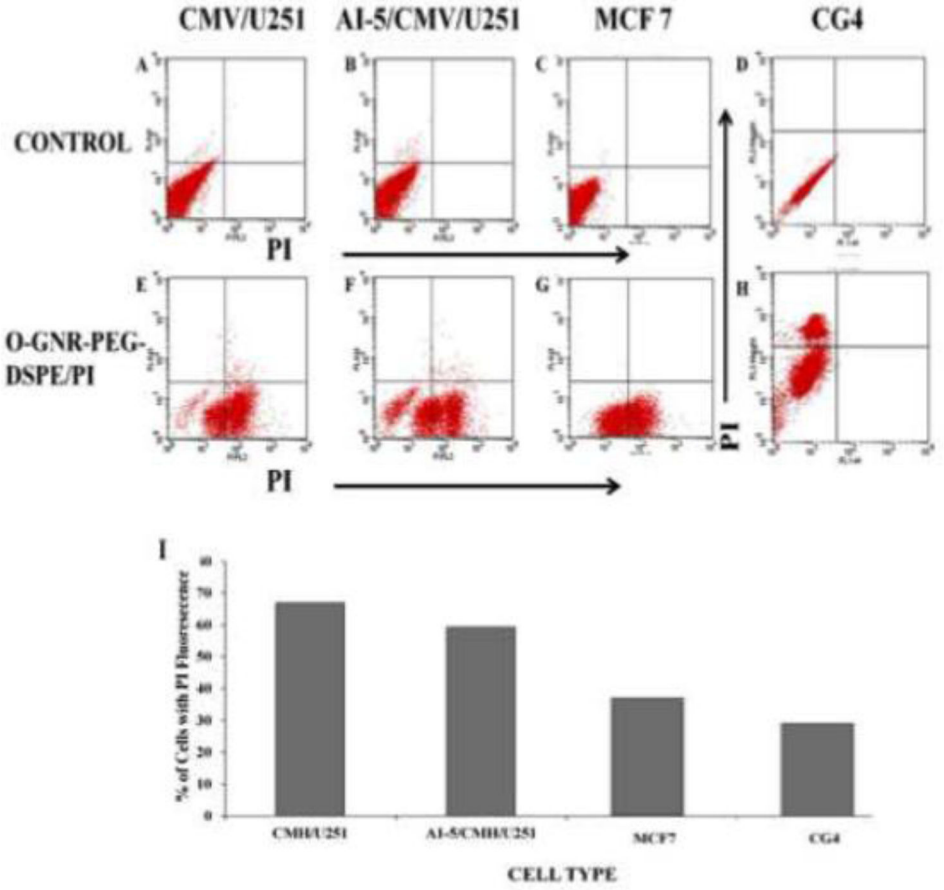

Figure 2.

Flow cytometry based analysis showing internalization of O-GNR-PEG-DSPE into GBM and CG-4 cell lines. CMV/U251 (A, D), A1-5/CMV/U251 cells (B, E) and CG-4 (C,F) were either left untreated as a control (A, B,C) or incubated with PI-loaded O-GNR-PEG-DSPEs for 24 h (D,E,F). After 24 h, ~67% and ~60% of CMV/U251 and A1-5/U251 respectively showed significant PI fluorescence, while ~29% of CG-4 showed significant fluorescence.

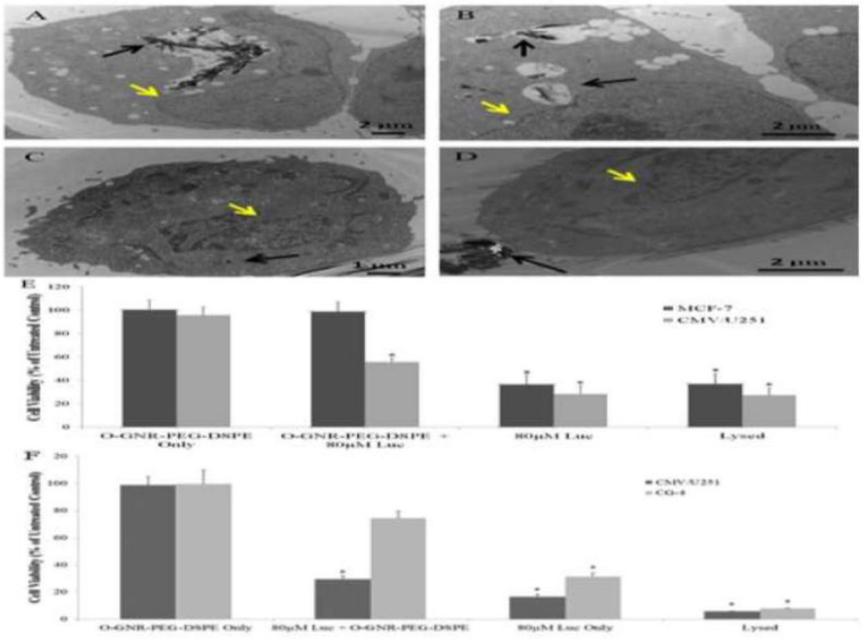

Figure 3.

Representative TEM images showing (A) Uptake of large aggregates of O-GNR-PEG-DSPE by CMV/U251 in large vesicular structures (indicated with black arrow) (B) Uptake of smaller O-GNR-PEG-DSPE aggregates into multiple vesicular structures in CMV/U251 (indicated with black arrow) (C) MCF-7 does not show high uptake of O-GNR-PEG-DSPE particles (only small aggregates were observed, indicated with black arrow) (D) Large aggregates did not get taken up my MCF-7 (indicated with black arrows). Both cell lines were exposed to 40μg/ml O-GNR-PEG-DSPE for 3 h. The nucleus in all cells is indicated in yellow. (E) PrestoBlue assay measuring viability of MCF-7 and CMV/U251 in co-culture conditions after being treated for 24 h with either O-GNR-PEG-DSPE, O-GNR-PEG-DSPE loaded with 80μM Luc, 80μM Luc, or lysis buffer. (*) indicates significant difference compared to untreated control (N=3). (F) PrestoBlue assay measuring viability of CG-4 and CMV/U251 in co-culture conditions after being treated for 24 h with either O-GNR-PEG-DSPE, O-GNR-PEG-DSPE loaded with 80μM Luc, 80μM Luc, or lysis buffer. (*) indicate significant difference compared to untreated control (N=3).

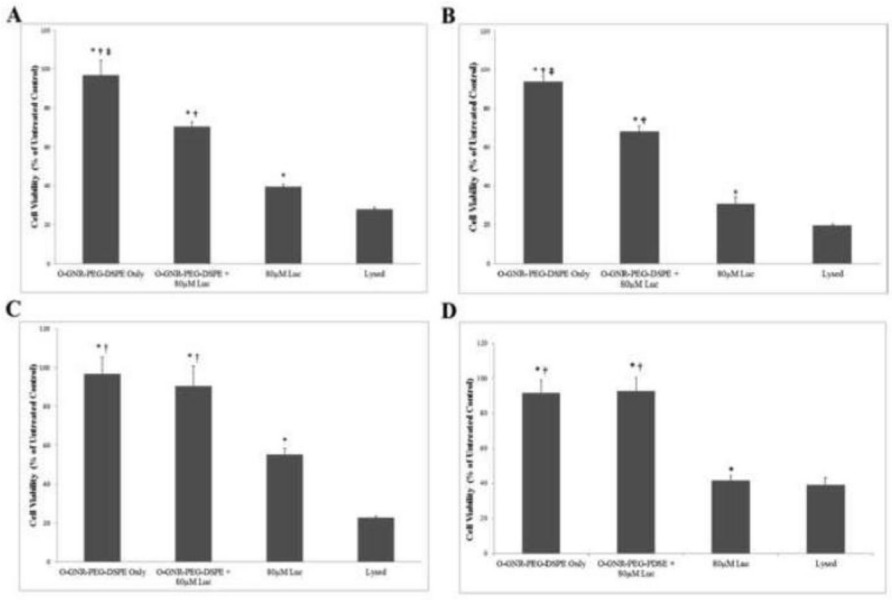

Figure 4.

PrestoBlue assay measuring viability of 5×10^3 CMV/U251 (A), A1-5 U251 (B) CG-4 (C) and MCF-7 (D) after being treated for 24 h with either O-GNR-PEG-DSPE, O-GNR-PEG-DSPE loaded with 80μM Luc, 80μM Luc, or lysis buffer. (*) indicates significance difference compared to lysis control, (†) indicates significant difference compared to 80μM Luc, and (‡) indicates significant difference compared to O-GNR-PEG-DSPE loaded with 80μM Luc.

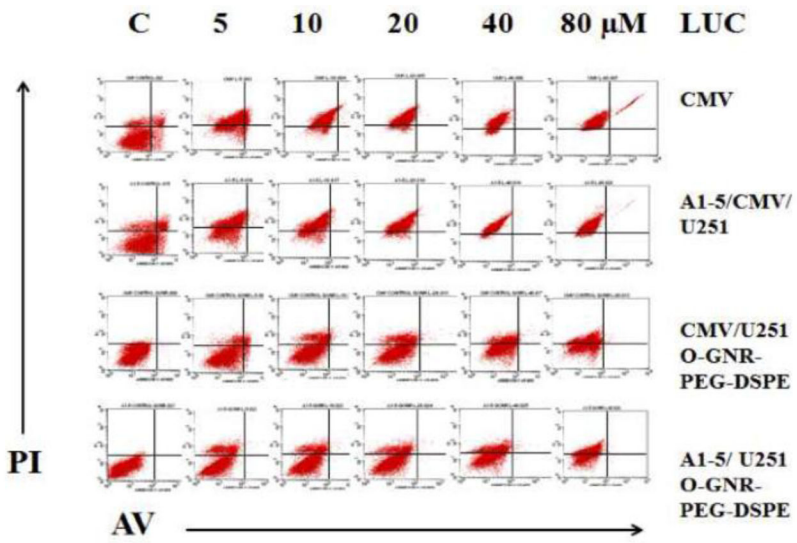

Figure 5.

Flow cytometry based analysis of cell death in control CMV/U251 and APE-1 overexpressor A1-5/CMV/U251 treated for 4 h with different concentrations of Luc (5–80 μM) either alone or loaded onto O-GNR-PEG-DSPE using AnnexinV/PI staining.

Table 1

Toxicity of lucanthone is reduced when coated on Graphene nanoribbons (O-GNR) in GBM cell line U251
Quantification of cells undergoing apoptosis and necrosis in Figure 5.

Cell Type	Lucanthone (μM)	% PI-AV-	% PI+	% Av+	% PI+AV+
CMV	C	79	10	4	6
	5	20	78	0	17
	10	5	95	0	0
	20	3	97	0	0
	40	3	97	0	0
	80	0	95	5	0
A1-5	C	72	15	3	10
	5	24	76	0	0
	10	8	92	0	0
	20	2	98	0	0
	40	0	100	0	0
	80	0	100	0	0
CMV/	GONR	C	96	0	0
	5	84	12	3	1
	10	77	23	0	0
	20	74	26	0	0
	40	52	48	0	0
	80	37	63	0	0
A1-5/	GONR	C	99	1	0
	5	77	23	0	0
	10	77	23	0	0
	20	76	24	0	0
	40	56	44	0	0
	80	43	57	0	0